

## Study of the interface stability of the metal (Mo, Ni, Pd)/HfO<sub>2</sub>/AlN/InGaAs MOS devices

Huy Binh Do, , Quang Ho Luc, , Minh Thien Huu Ha, , Sa Hoang Huynh, , Tuan Anh Nguyen, , Yueh Chin Lin, and , and Edward Yi Chang

Citation: *AIP Advances* **7**, 085208 (2017); doi: 10.1063/1.4986147

View online: <http://dx.doi.org/10.1063/1.4986147>

View Table of Contents: <http://aip.scitation.org/toc/adv/7/8>

Published by the [American Institute of Physics](#)

---

### Articles you may be interested in

[Single step vacuum-free and hydrogen-free synthesis of graphene](#)

*AIP Advances* **7**, 085301 (2017); 10.1063/1.4985751

[Grain growth mechanism and magnetic properties in L1<sub>0</sub>-FePt thin films](#)

*AIP Advances* **7**, 085203 (2017); 10.1063/1.4991423

[Improved efficiency of organic solar cells using Au NPs incorporated into PEDOT:PSS buffer layer](#)

*AIP Advances* **7**, 085302 (2017); 10.1063/1.4995803

[Counterevidence to the ion hammering scenario as a driving force for the shape elongation of embedded nanoparticles](#)

*AIP Advances* **7**, 085304 (2017); 10.1063/1.4993251

[Angular distribution of hybridization in sputtered carbon thin film](#)

*AIP Advances* **7**, 085303 (2017); 10.1063/1.4990858

---

# HAVE YOU HEARD?

Employers hiring scientists and engineers trust

**PHYSICS TODAY | JOBS**

[www.physicstoday.org/jobs](http://www.physicstoday.org/jobs)



## Study of the interface stability of the metal (Mo, Ni, Pd)/HfO<sub>2</sub>/AlN/InGaAs MOS devices

Huy Binh Do,<sup>1</sup> Quang Ho Luc,<sup>1</sup> Minh Thien Huu Ha,<sup>1</sup> Sa Hoang Huynh,<sup>1</sup> Tuan Anh Nguyen,<sup>1</sup> Yueh Chin Lin,<sup>1</sup> and Edward Yi Chang<sup>1,2,3,a</sup>

<sup>1</sup>Department of Materials Science and Engineering, National Chiao Tung University, 1001 University Road, Hsinchu 300, Taiwan

<sup>2</sup>Department of Electronics Engineering, National Chiao Tung University, 1001 University Road, Hsinchu 300, Taiwan

<sup>3</sup>International College of Semiconductor Technology, National Chiao Tung University, 1001 University Road, Hsinchu 300, Taiwan

(Received 24 April 2017; accepted 31 July 2017; published online 9 August 2017)

The degeneration of the metal/HfO<sub>2</sub> interfaces for Mo, Ni, and Pd gate metals was studied in this paper. An unstable PdO<sub>x</sub> interfacial layer formed at the Pd/HfO<sub>2</sub> interface, inducing the oxygen segregation for the Pd/HfO<sub>2</sub>/InGaAs metal oxide capacitor (MOSCAP). The low dissociation energy for the Pd-O bond was the reason for oxygen segregation. The PdO<sub>x</sub> layer contains O<sup>2-</sup> and OH<sup>-</sup> ions which are mobile during thermal annealing and electrical stress test. The phenomenon was not observed for the (Mo, Ni)/HfO<sub>2</sub>/InGaAs MOSCAPs. The results provide the guidance for choosing the proper metal electrode for the InGaAs based MOSFET. © 2017 Author(s). All article content, except where otherwise noted, is licensed under a Creative Commons Attribution (CC BY) license (<http://creativecommons.org/licenses/by/4.0/>). [<http://dx.doi.org/10.1063/1.4986147>]

Hafnium-based oxides are recently considered as promising candidates as the high-k dielectric for III-V channel devices.<sup>1-6</sup> The HfO<sub>2</sub>/InGaAs interface, which affects the power consumption of complementary metal-oxide-semiconductor (CMOS), has been greatly improved recently.<sup>7,8</sup> The reactions between the metal electrode and the oxide layer may lead to the degeneration of the oxide layer. To prevent these interface reactions, the multilayer metal alloy of TiNi was used as the gate electrode for the HfO<sub>2</sub>/InGaAs metal oxide semiconductor capacitor (MOSCAP).<sup>9</sup> Also, a thin AlN layer was inserted between the metal electrode and the HfO<sub>2</sub> layer to suppress this interface reactions.<sup>10</sup> Yoshida et al.<sup>11</sup> recently reported that the reactions between the high-k material and InGaAs were due to the interaction at the metal/oxide interface. Their study indicated that the metal electrode affects not only on the metal/HfO<sub>2</sub> interface but also on the HfO<sub>2</sub>/InGaAs interface. To suppress this interfacial interaction, the passivation of HfO<sub>2</sub>/InGaAs interface using AlN layer was reported.<sup>7,12</sup> Therefore, the mechanism suggested by Yoshida et al. should be complemented when a non-oxide layer is used to passivate the HfO<sub>2</sub>/InGaAs interface. Additionally, the oxide degeneration depends not only on the electrode-high-k reaction but also on the inter diffusion between the oxide layer and the metal electrode after post metal-deposition annealing (PMA). In this study, the oxygen segregation at the (Mo, Ni, Pd)/HfO<sub>2</sub> interfaces of the HfO<sub>2</sub>/AlN/InGaAs MOSCAP is investigated. Mo was chosen due to its low work function applicable for NMOS InGaAs devices, while Ni and Pd were chosen because of their high work function suitable for PMOS InGaAs devices.

The MOSCAP was fabricated on the 100-nm epitaxial In<sub>0.53</sub>Ga<sub>0.47</sub>As layer ( $5 \times 10^{17}/\text{cm}^3$  Si-doped n-type wafer) which was grown on the n+-InP substrate (using molecular beam epitaxial (MBE) growth technique). First, the wafer went through an HCl:H<sub>2</sub>O (3.8%) solution treatment for 2 minutes before it was loaded into the ALD chamber. Then, 0.8-nm AlN layer and 50 cycles HfO<sub>2</sub> were deposited on the InGaAs layer.<sup>13</sup> The AlN layer serves as the passivation layer to prevent the

<sup>a</sup>Author to whom correspondence should be addressed. Electronic mail: [edc@mail.nctu.edu.tw](mailto:edc@mail.nctu.edu.tw)



reaction between oxygen atoms in  $\text{HfO}_2$  and In, Ga, and As atoms in the InGaAs channel.<sup>7</sup> After that, the samples were annealed in forming gas (FG) at 450 °C for 5 minutes using rapid thermal annealing (RTA). Three types of metal including Mo, Ni, and Pd (with the same thickness of 50 nm) were studied as the gate metals on the  $\text{HfO}_2$  layer. The gate metals were deposited through E-gun evaporation with the based pressure about  $3 \times 10^{-7}$  torr. The deposition rate was controlled by quartz crystals (gold, 6 MHz) and kept to be 1 Å/s. The AuGeNiAu was deposited on the backside of the wafer to form the ohmic contact. Finally, the MOSCAPs were annealed in three different ambiances including FG, nitrogen (N) and oxygen (O) at 350 °C for 30s using RTA for comparison. The metal/ $\text{HfO}_2$  interfaces were characterized by using a Field Emission High-resolution transmission electron microscopy (HRTEM) JEM-2100F, while the thickness of  $\text{HfO}_2$  was determined by using a SOPRA GES5 Ellipsometer and confirmed by HRTEM measurement. The capacitance-voltage (C-V) and current-voltage (J-V) were performed by using an HP4284A LCR meter. The X-ray photoelectron spectroscopic (XPS) were measured in a commercial Microlab 350 XPS system with Al  $K\alpha$  source. The core levels were determined by using XPSPEAK (version 4.1) with Gaussian-Lorentz line shape and a Shirley background. Sample charging effects were corrected by placing the Au  $4f_{7/2}$  peak at binding energy of 84.0 eV and shifting the rest of the regions accordingly. The uncertainty of the core position was 0.05 eV.

Figure 1(a) shows the capacitance-voltage hysteresis ( $\Delta V_{\text{FB}}$ ) of the (Mo, Ni, Pd)/ $\text{HfO}_2/\text{AlN}/\text{InGaAs}$  MOSCAPs. The flat band voltage ( $V_{\text{FB}}$ ) was determined from the comparative method.<sup>14</sup> The fact that the  $\Delta V_{\text{FB}}$  of the Pd MOSCAP is very large ( $\sim 1$  V), while the  $\Delta V_{\text{FB}}$  of the Mo MOSCAP is very small ( $\sim 0.11$  V) indicates that a large number of bulk oxide traps were created after Pd was deposited on  $\text{HfO}_2$  and annealed in FG. The large  $\Delta V_{\text{FB}}$  was due to the interaction of Pd atoms and O atoms at the Pd/ $\text{HfO}_2$  interface, which creates oxygen vacancies inside the  $\text{HfO}_2$  layer. This reaction leads to the increase of the oxide thickness and reduces the accumulation capacitance ( $C_{\text{acc}}$ ) of the Pd MOSCAP as shown in Fig. 1(b). Based on the thermodynamics, the  $\Delta C_{\text{acc}}$  of the Mo MOSCAP should be larger than the  $\Delta C_{\text{acc}}$  of the Pd MOSCAP because the Mo-O reaction (oxidation formation enthalpy  $\Delta H \sim -178$  kCal/mol) is more exothermal than the Pd-O reaction ( $\Delta H - 49.9$  kCal/mol).<sup>15</sup> However, the opposite results were observed in Fig. 1(b), indicating that the oxidation at the Pd/ $\text{HfO}_2$  interface is not the only reason for the oxide degeneration for the Pd/ $\text{HfO}_2/\text{AlN}/\text{InGaAs}$  MOSCAP. Instead, an unstable IL  $\text{PdO}_x$  at the Pd/ $\text{HfO}_2$  interface should attribute to the oxygen segregation at the Pd/ $\text{HfO}_2$  gate stack. Fig. 1(c) and 1(d) show the leakage currents and the  $D_{\text{it}}$ , respectively, for the three MOSCAPs. The leakage currents of the three MOSCAPs were in the range of  $2 \times 10^{-8}$  A/cm<sup>2</sup>  $\sim 6 \times 10^{-8}$  A/cm<sup>2</sup>, indicating that the  $\text{HfO}_2/\text{InGaAs}$  interface was totally passivated by AlN IL layer.<sup>6,7</sup>

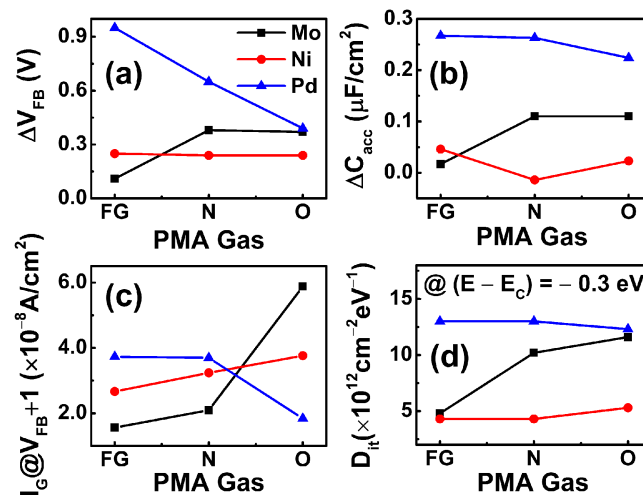


FIG. 1. The electrical characteristics of (Mo, Ni, Pd)/ $\text{HfO}_2/\text{AlN}/\text{InGaAs}$  MOSCAPs after PMA in FG, N and O ambient gases at 350 °C for 30s, (a) the hysteresis at  $V_{\text{FB}}$  of the C-V curves after PMA, (b) the  $C_{\text{acc}}$  variation of the MOSCAPs after PMA measured at +2 V and 1MHz, (c) the leakage currents at  $V_{\text{FB}} + 1$  (V) after PMA, and (d) the  $D_{\text{it}}$  at  $E - E_c = -0.3$  eV from the conduction band edge after PMA.

The low  $D_{it}$  values ( $\sim 4 \times 10^{12} \text{ cm}^{-2} \text{ eV}^{-1}$  determined from Terman method<sup>16</sup>) of the Ni MOSCAP and the Mo MOSCAP, shown in Fig. 1(d), are in agreement with the previous reports.<sup>6,7,10</sup> Note that Terman method gives both slow and fast traps and provides a reliable value for  $D_{it}$  at mid-gap.<sup>16</sup> The In out-diffusion<sup>9,17-20</sup> from InGaAs substrate to the oxide layer ( $\text{Al}_2\text{O}_3$  or  $\text{HfO}_2$ ) was also reported to affect the quality of the oxide layer. The  $D_{it}$  values of Pd MOSCAPs are much higher than those of Ni and Mo MOSCAPs as shown in Fig. 1(d), indicating that the  $\text{PdO}_x$  layer at Pd/ $\text{HfO}_2$  interface reduces the passivation effects of AlN layer. The increase of oxygen vacancies inside  $\text{HfO}_2$  due to the reaction of Pd and  $\text{HfO}_2$  may facilitate the out-diffusion of In atoms from InGaAs substrate to  $\text{HfO}_2$  layer, leading to the increase of  $D_{it}$  for the Pd MOSCAPs. Fig. 1 also shows that the PMA process has little effect on the electrical characteristics of the Ni MOSCAP; thus, Ni is a more suitable gate metal for the InGaAs based p-MOSFET.<sup>7</sup>

The dissociation energies ( $D_S$ ) of the metal-oxygen bonds for the metals used in this study are Mo-O bond (119.9 kCal/mol), Ni-O bond (87.42 kCal/mol), and Pd-O bond (53.87 kCal/mol).<sup>21</sup> It can be seen that  $\text{PdO}_x$  is easier to decompose during the PMA process compared to other oxides in this study following the equation:



The  $\text{O}^{2-}$  ions can easily diffuse into the Pd layer, leading to the formation of a thick  $\text{PdO}_x$  IL at the Pd/ $\text{HfO}_2$  interface as shown in Fig. 2(a). This IL was not found at the Ni/ $\text{HfO}_2$  interface as shown in Fig. 2(b). Fig. 2(c) shows the Energy-dispersive X-ray spectroscopy (EDS) spot profile of the  $\text{PdO}_x$  IL. An oxygen percent of  $\sim 24\%$  was found in the  $\text{PdO}_x$  layer, indicating a significant internal diffusion of the  $\text{O}^{2-}$  ions from the  $\text{HfO}_2$  layer into the Pd layer. Fig. 2(d) and (e) show the scanning electron microscope (SEM) images of the Pd MOSCAP and the Ni MOSCAP, respectively, after RTA in FG at 400 °C for 5 minutes. Some bubbles occurred at the surface of the Pd MOSCAP, indicating that the Pd MOSCAP was destroyed due to the diffusion of  $\text{O}^{2-}$  ions from the  $\text{HfO}_2$  layer into the Pd layer.

To investigate the stability of the  $\text{PdO}_x$  IL due to the oxygen segregation at the  $\text{HfO}_2$  layer, the XPS analysis was conducted on the clean  $\text{HfO}_2$  surface, the (2-nm) Mo/ $\text{HfO}_2$  interface, and the (2-nm) Pd/ $\text{HfO}_2$  interface; the results are shown in Fig. 3. For the clean  $\text{HfO}_2$  surface, the XPS data is shown in Fig. 3(a). The strongest peak  $\text{O}^I$  (530.57 eV) is attributed to the oxygen in a metal-oxygen bond without oxygen vacancy; the peak  $\text{O}^{II}$  (532.54 eV) and the peak  $\text{O}^{III}$  (533.83 eV) are attributed to the oxygen in the metal-oxygen bond with oxygen vacancy and the OH group attached to Hf<sup>2+</sup> ions, respectively.<sup>22</sup> The O 1s peak of the Mo/ $\text{HfO}_2$  interface after PMA in FG at 350 °C for 30s is same as the O 1s peak of the clean  $\text{HfO}_2$  surface, indicating that the Mo/ $\text{HfO}_2$  interface is quite stable due to the large dissociation energy of the Mo-O bond. For the Pd/ $\text{HfO}_2$  interface, due to the overlap of the Pd 3p<sub>3/2</sub> peak with the O 1s peaks, the Pd 3p<sub>1/2</sub> peak was firstly set at 562.20 eV<sup>23</sup> as a standard for the Pd 3p<sub>3/2</sub>,  $\text{O}^I$ ,  $\text{O}^{II}$ , and  $\text{O}^{III}$  peaks fitting. The spin-orbit splitting of the Pd 3p peak was chosen at 27.8 eV, which was in agreement with the previous report.<sup>24</sup> It was found that the  $\text{O}^I$  intensity decreased from 85.4 % for the clean  $\text{HfO}_2$  surface to 33 % for the Pd/ $\text{HfO}_2$  interface as shown in Table I. The considerable increase of the intensities of the  $\text{O}^{II}$  and  $\text{O}^{III}$  peaks at the Pd/ $\text{HfO}_2$  interface indicates a significant increase of the oxygen vacancies in  $\text{HfO}_2$ , due to the diffusion of  $\text{O}^{2-}$  ions from the  $\text{HfO}_2$  layer to the Pd layer. The same phenomenon was observed in Fig. 3(b). The intensity of the Pd 4d peak ( $\sim 1.4$  eV) clearly decreased after the Pd/ $\text{HfO}_2$  interface was annealed in FG at 350 °C for 30s, while the intensity of O 2p peak ( $\sim 7$  eV) increased after the sample was annealed. The Hf 4f peaks shifted after Pd deposition on the  $\text{HfO}_2$  surface; this shift was due to the metal induced gap state phenomenon<sup>25</sup> at the Pd/ $\text{HfO}_2$  interface. After the Pd MOSCAP was annealed, the increases of the  $\text{O}^{2-}$  and  $\text{OH}^-$  ion densities, as can be seen in Fig. 3(a), induced a dipole at the Pd/ $\text{HfO}_2$  interface which increased the binding energy of Hf 4f peak as shown in Fig. 3(b).

Figures 4(a) and (b) show the C-V characteristics of the Pd MOSCAP and the Mo MOSCAP, respectively, with the gate stress at  $-2$  V and  $+2$  V for 1800s; the C-V behavior can be used to investigate the effects of the  $\text{O}^{2-}$  and  $\text{OH}^-$  ions diffusion on the oxide film. To track the degeneration of the oxide layer due to a movement of the  $\text{O}^{2-}$  and  $\text{OH}^-$  ions, the C-V measurements were suddenly conducted during the constant-voltage-stress.<sup>26,27</sup> For the Pd MOSCAP, the C-V curve was found to have negative shift, and the  $C_{acc}$  was found to increase after it went through the negative stress

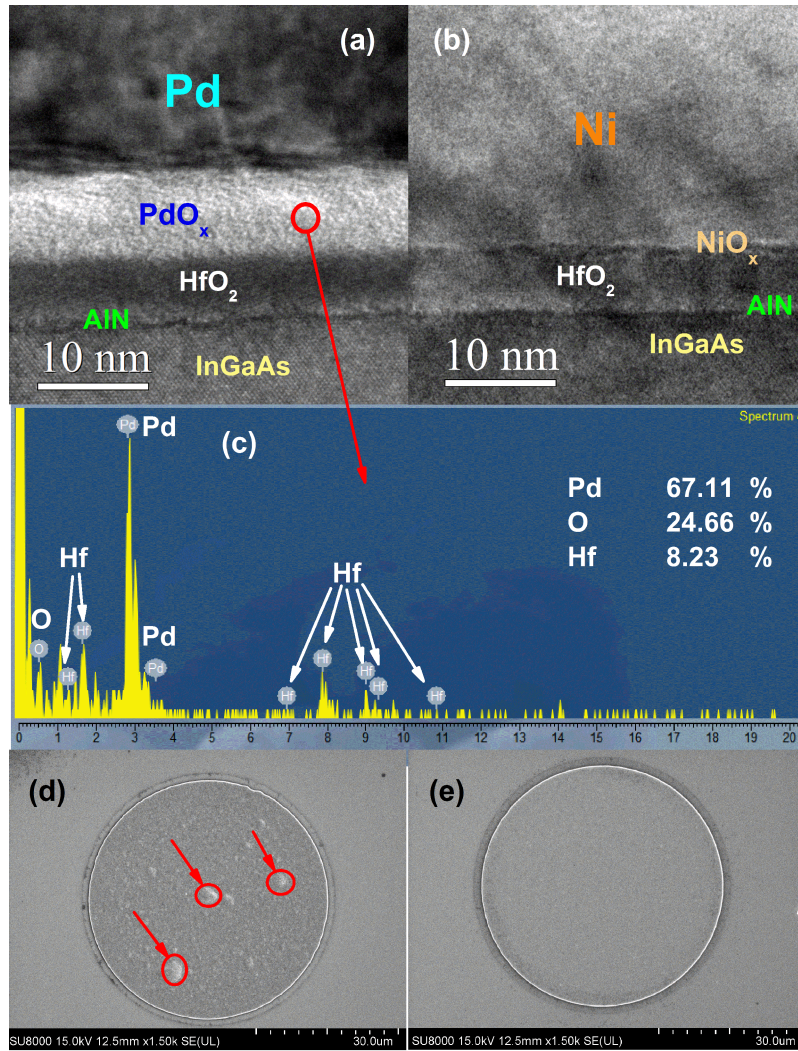


FIG. 2. (a) and (b) TEM cross sections of Pd/HfO<sub>2</sub>/AlN/InGaAs and Ni/HfO<sub>2</sub>/AlN/InGaAs structures after RTA in FG at 350 °C for 30s, respectively, (c) the EDS spot profile of the interfacial layer PdO<sub>x</sub> at the Pd/HfO<sub>2</sub> interface, (d) and (e) SEM images of the patterns of Pd/HfO<sub>2</sub> and Ni/HfO<sub>2</sub> MOSCAPs, respectively, after RTA in FG at 400 °C for 5 minutes.

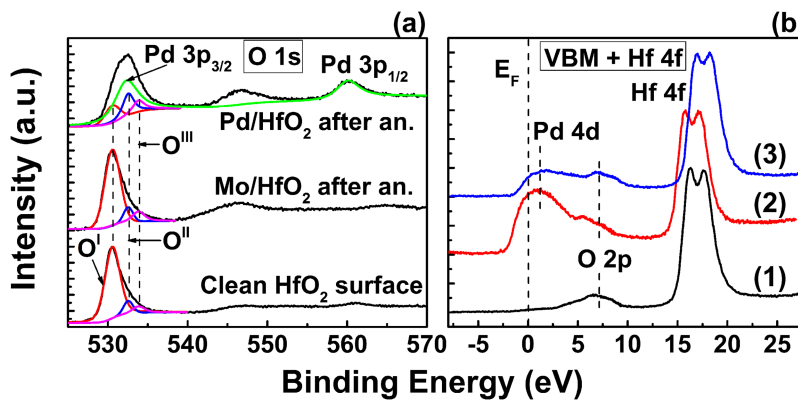


FIG. 3. XPS spectra of (a) O 1s peaks of clean HfO<sub>2</sub> surface, Mo/HfO<sub>2</sub> and Pd/HfO<sub>2</sub> interfaces after PMA in FG at 350 °C for 30s, (b) valence band maximum (VBM) and Hf 4f peaks of (1) clean HfO<sub>2</sub> surface, (2) Pd/HfO<sub>2</sub> interface as deposited and (3) Pd/HfO<sub>2</sub> interface after PMA in FG at 350 °C for 30s.

TABLE I. The area percent (%) of  $O^I$ ,  $O^{II}$ , and  $O^{III}$  peaks of clean  $HfO_2$  surface, Mo/ $HfO_2$  interface and Pd/ $HfO_2$  interface.

$O^i/(O^I+O^{II}+O^{III})$	Clean $HfO_2$	Mo/ $HfO_2$	Pd/ $HfO_2$
$O^I$	85.4	79.8	33.0
$O^{II}$	8.5	9.5	41.7
$O^{III}$	6.1	10.7	25.3

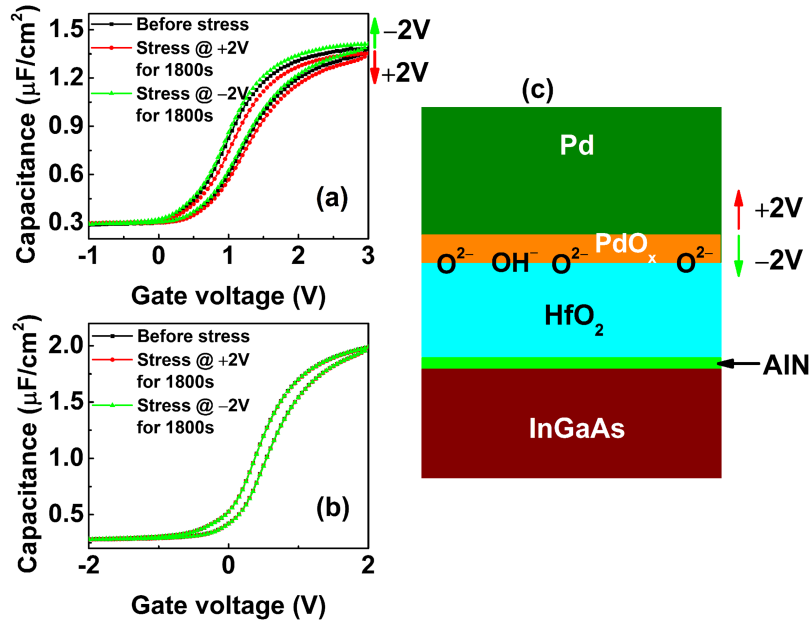


FIG. 4. The effects of  $O^{2-}$  and  $OH^-$  ions on the C-V behaviors of Pd MOSCAP and Mo MOSCAP, (a) and (b) the C-V characteristics of Pd MOSCAP and Mo MOSCAP, respectively, after gate stressed at  $-2$  V and  $+2$  V for 1800s; (c) the schematic  $PdO_x$  interfacial layer after gate stressed at  $-2$  V and  $+2$  V for 1800s.

(at  $-2$  V). The negative stress reduced the densities of the  $O^{2-}$  and  $OH^-$  ions, leading to the reduction of the  $PdO_x$  thickness and the negative shift of the C-V curve. After the positive stress (at  $+2$  V), the opposite phenomenon appeared with the positive shift of the C-V curves and the reduction of  $C_{acc}$ . The effect of the voltage stress on the  $PdO_x$  layer is illustrated in Fig. 4(c). For the Mo MOSCAP, the C-V curve shift and the  $C_{acc}$  reduction were not found, as shown in Fig. 4(b). The results indicate that the stable Mo-O and Ni-O bonds can prevent the oxygen segregation at the (Mo, Ni)/ $HfO_2$  interfaces. However, for the Pd/ $HfO_2$  case, the unstable Pd-O bond (with very low  $D_S$ ) favors the oxygen segregation at the Pd/ $HfO_2$  interface, leading to the increase of the thickness of the  $PdO_x$  layer as shown in Fig. 2(a) and the oxygen vacancies in the  $HfO_2$  film as shown in Fig. 3(a).

The stability of the (Mo, Ni, Pd)/ $HfO_2$  interfaces is investigated for low power consumption InGaAs based MOS device applications in this study. The oxidations at the Mo/ $HfO_2$  and the Ni/ $HfO_2$  interfaces were found to have no effect on the quality of the gate stack; however, the formation of the interfacial layer  $PdO_x$  at the Pd/ $HfO_2$  interface considerably increased the oxygen vacancies in the  $HfO_2$  film. The unstable  $PdO_x$  layer contains the  $O^{2-}$  and  $OH^-$  ions, which are mobile during annealing and the electrical stress test. The results demonstrate that the dissociation energy of the metal-oxygen bond and the enthalpy of formation of the metal oxide should be considered when choosing the right gate metal for the InGaAs MOSFET devices.

This work was sponsored by the TSMC, NCTU-UCB I-RiCE program, and Ministry of Science and Technology, Taiwan, under Grant No. MOST 106-2911-I-009-301 and National Chung-Shan Institute of Science & Technology, Taiwan, under Grant No. NCSIST-103-V312(106).

- <sup>1</sup> J. A. del Alamo, *Nature* **479**(7373), 317 (2011).
- <sup>2</sup> S. A. Baig, J. L. Boland et al., *Nano Letters* **17**(4), 2603 (2017).
- <sup>3</sup> J. Cheol Shin, K. Hyun Kim et al., *Nano Letters* **11**(11), 4831 (2011).
- <sup>4</sup> C. Zhang and X. Li, *IEEE Transactions on Electron Devices* **63**(1), 223 (2016).
- <sup>5</sup> Y. Han, Q. Li et al., *Applied Physics Letters* **108**(24), 242105 (2016).
- <sup>6</sup> Q. H. Luc, S. P. Cheng et al., *IEEE Electron Device Letters* **37**(8), 974 (2016).
- <sup>7</sup> H. B. Do, Q. H. Luc et al., *IEEE Transactions on Electron Devices* **62**(12), 3987 (2015).
- <sup>8</sup> V. Chobpattana, E. Mikheev et al., *Journal of Applied Physics* **116**(12), 124104 (2014).
- <sup>9</sup> H. B. Do, Q. H. Luc et al., *IEEE Transactions on Electron Devices* **63**(12), 4714 (2016).
- <sup>10</sup> H. B. Do, Q. H. Luc et al., *IEEE Electron Device Letters* **38**(5), 552 (2017).
- <sup>11</sup> S. Yoshida, D. Lin et al., *Applied Physics Letters* **109**(17), 172101 (2016).
- <sup>12</sup> Q. H. Luc, H. B. Do et al., *IEEE Electron Device Letters* **36**(12), 1277 (2015).
- <sup>13</sup> Q. H. Luc, E. Y. Chang et al., *IEEE Transactions on Electron Devices* **61**(8), 2774 (2014).
- <sup>14</sup> H. B. Do, Q. H. Luc et al., *IEEE Electron Device Letters* **37**(9), 1100 (2016).
- <sup>15</sup> A. A. Demkov, *Physical Review B* **74**(8), 085310 (2006).
- <sup>16</sup> R. Engel-Herbert, Y. Hwang et al., *Journal of Applied Physics* **108**(12), 124101 (2010).
- <sup>17</sup> I. Krylov, R. Winter et al., *Applied Physics Letters* **104**(24), 243504 (2014).
- <sup>18</sup> I. Krylov, A. Gavrilov et al., *Applied Physics Letters* **103**(5), 053502 (2013).
- <sup>19</sup> A. Sanchez-Martinez, O. Ceballos-Sanchez et al., *Journal of Applied Physics* **114**(14), 143504 (2013).
- <sup>20</sup> W. Cabrera, B. Brennan et al., *Applied Physics Letters* **104**(1), 011601 (2014).
- <sup>21</sup> W. M. Haynes, (CRC Press, Milton, 2016).
- <sup>22</sup> P. K. Nayak, Z. Wang et al., *Applied Physics Letters* **106**(10), 103505 (2015).
- <sup>23</sup> M. C. Militello and S. J. Simko, *Surface Science Spectra* **3**(4), 387 (1994).
- <sup>24</sup> P. M. Th M. van Attekum and J. M. Trooster, *Journal of Physics F: Metal Physics* **9**(11), 2287 (1979).
- <sup>25</sup> J. Tersoff, *Physical Review Letters* **52**(6), 465 (1984).
- <sup>26</sup> F. Palumbo and M. Eizenberg, *Journal of Applied Physics* **115**(1), 014106 (2014).
- <sup>27</sup> J. Franco, A. Alian et al., presented at the 2014 IEEE International Reliability Physics Symposium, 2014 (unpublished).